

MATHEMATICAL MODELING OF FOG WATER DEPOSITION,  
SAN FRANCISCO, CALIFORNIA

AS  
36  
2014  
GEOL  
•C67

A thesis submitted to the faculty of  
San Francisco State University  
In partial fulfillment of  
the requirements for  
the Degree

Master of Science

In

Geoscience

by

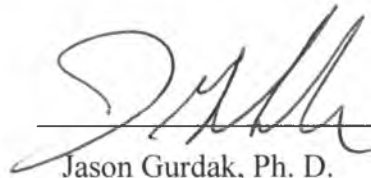
Ryan Michael Corbett

San Francisco, California

Spring 2014

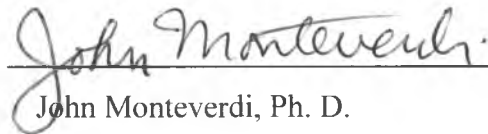
CERTIFICATION OF APPROVAL

I certify that I have read *Mathematical Modeling of Fog Water Deposition*, San Francisco, California by Ryan Michael Corbett, and that in my opinion this work meets the criteria for approving a thesis submitted in partial fulfillment of the requirement for the degree Master of Science in Geoscience at San Francisco State University.



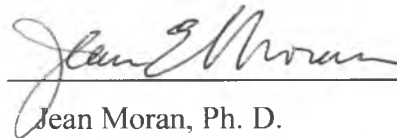
Jason Gurdak, Ph. D.

Assistant Professor of Geoscience



John Monteverdi, Ph. D.

Professor of Geoscience



Jean Moran, Ph. D.

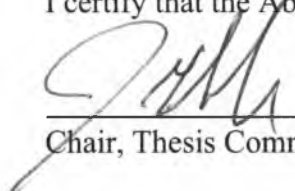
Associate Professor of Geoscience

MATHEMATICAL MODELING OF FOG WATER DEPOSITION, SAN  
FRANCISCO, CALIFORNIA

Ryan Michael Corbett  
San Francisco, California  
2014

Fog drip is a liquid form of occult precipitation that occurs when fog moves through vegetation and fog droplets are deposited on the vegetative surfaces and the water drips to the ground. Fog drip is an important hydrologic input to many ecosystems, including those in the San Francisco Bay Area where a number of studies have quantified fog drip and fog deposition from manmade collectors, which are a good approximation of fog drip. This is the first study to examine the correlation between meteorological conditions during advection fog episodes in the San Francisco Bay Area as well as fog deposition volume and stable isotopic composition. Meteorological data and fog deposition samples from a standard fog collector (SFC) and harp design were collected for a three-month period (2012) at a coastal site in Fort Funston, which is part of the Golden Gate National Recreation Area. Fog deposition samples from the SFC and harp collector were not significantly independent with mean  $\delta D$  and  $\delta^{18}O$  values,  $-13.74$  (standard deviation  $0.80$ ) and  $-2.63$  (standard deviation  $0.15$ ), respectively. These results support the important finding that fractionation of fog deposition is not a function of fog collector design. Meteorological data, fog deposition volume, and isotopic composition were used to construct multivariate linear regression models. Fog deposition volume strongly correlated with event duration, relative humidity, temperature, and wind direction, while isotopic composition strongly correlated with relative humidity and wind direction data.

I certify that the Abstract is a correct representation of the content of this thesis

  
\_\_\_\_\_  
Chair, Thesis Committee

5-13-2014  
\_\_\_\_\_  
Date

## ACKNOWLEDGEMENT

First and foremost, I would like to thank Jason Gurdak for his guidance throughout my coursework at San Francisco State University. I am indebted to his help and I cannot thank him enough for his patience and optimism throughout my research. I would also like to acknowledge my committee members John Monteverdi and Jean Moran for their support and advice. Special thanks go to Zach Lauffenburger, Mike Wrigley, and Zi Zi Searles for helping me find laughter at every roadblock. Special thanks go to my friends and family, and a very special thank you to Nicole Van Cleave for the unwavering emotional support.

David and Doris Dawdy provided partial funding for this research. I applaud their generosity and lifelong dedication to deepening the understanding of our beautiful planet. Thank you the National Park Service for granting me permission to collect fog at Fort Funston. Finally, I would like to thank Leonard Sklar for giddy enthusiasm for large data sets and his eagerness to make sense of them. Without his help, this project would still be looking for a direction to take.

## TABLE OF CONTENTS

LIST OF TABLES.....	vi
LIST OF FIGURES .....	vii
1.0 Introduction.....	1
2.0 Study Area.....	5
3.0 Methods.....	7
3.1 Fog Deposition Collectors and Meteorological Instrumentation .....	7
3.2 Isotope Analysis of Fog Deposition.....	8
3.3 Modeling Fog Deposition Volume.....	8
3.4 Modeling Fog Deposition Isotopes .....	9
4.0 Results.....	10
4.1 Fog Deposition and Meteorological Data .....	10
4.2 Isotope Geochemistry of Fog Deposition.....	11
4.3 Fog Deposition Volume Model.....	12
4.4 Fog Deposition Isotopic Model.....	13
5.0 Discussion.....	13
5.1 Fog Deposition and Meteorological Data .....	13
5.2 Isotope Geochemistry of Fog Deposition.....	15
5.3 Fog Deposition Volume Model.....	15
5.4 Fog Deposition Isotope Model.....	17
6.0 Conclusions .....	18
7.0 References .....	20

## LIST OF TABLES

Table 1: Fog event duration, total fog deposition volume, and calculated fog deposition.....	34
Table 2: Summary statistics of wind speed .....	36
Table 3: Summary statistics of wind direction .....	37
Table 4: Summary statistics of air temperature .....	38
Table 5: Summary statistics of Fog Potential Index (FPI) .....	39
Table 6: Stable isotope data .....	40
Table 7: Summary of explanatory variables for fog deposition model.....	41
Table 8: Multivariate linear regression model outputs for fog deposition volume....	41
Table 9: Summary of analysis explanatory variables for $\delta D$ model.....	41
Table 10: Summary of analysis of explanatory variables for $\delta^{18}O$ model.....	42
Table 11: Multivariate linear regression model outputs for $\delta^2H$ and $\delta^{18}O$ .....	42

## LIST OF FIGURES

Figure 1: Collection site and instrumentation at Fort Funston, CA.....	23
Figure 2: Location of Fort Funston, CA.....	24
Figure 3: Fog deposition volume.....	25
Figure 4: Hourly wind speed.....	26
Figure 5: Hourly average wind direction .....	27
Figure 6: Hourly air temperature .....	28
Figure 7: Hourly Fog Potential Index (FPI) .....	29
Figure 8: Total fog deposition volume and Fog Potential Index (FPI) .....	30
Figure 9: Stable isotopic compositions of fog water .....	31
Figure 10: Boxplots of $\delta^2\text{H}[\text{H}_2\text{O}]$ and $\delta^{18}\text{O}[\text{H}_2\text{O}]$ .....	32
Figure 11: Deuterium excess and wind direction .....	33

## 1.0 Introduction

Fog droplets that blow over the surfaces of plants and coalesce into drops large enough to fall to the ground are known as fog drip (Ingraham and Matthews, 1988), which can be an important hydrologic input to ecosystems (Ingraham and Matthews, 1995; Dawson 1998). Fog drip is a type of occult precipitation that is particularly important to the Californian redwood ecosystem (Dawson 1998; Burgess and Dawson, 2004) near the San Francisco Bay Area (hereafter referred to as Bay Area). The Mediterranean climate of the Bay Area is well known for thick diurnal advection fog that is a characteristic feature of the summer weather pattern. The majority of precipitation in the Bay Area falls between November and April, whereas the period May through October is dominated by coastal fog and stratus regimes with little to no rainwater precipitation from migratory storm systems or thunderstorms (Azevedo and Morgan, 1974; Hilliker and Fritsch, 1999). Fog in the Bay Area has long been long studied because it is an important meteorological feature in the Bay Area (Means, 1927; Byers, 1953; Oberlander, 1956; Goodman, 1977) and because it provides substantial hydrologic input (Ingraham and Matthehews, 1995; Dawson, 1998) and reduces the number of hours of direct sun, limiting the amount of diurnal evapotranspiration (Byers, 1953).

To quantify that amount of fog drip, researchers have used rain gauges positioned under trees that intercept passing fog. For example, Oberlander (1956) reported daily fog

drip rates ranging between 1.2–37 mm/day over a 40-day period along Cahill Ridge, San Mateo County in the Bay Area. The movement of fog drip through the hydrosphere has also been traced using stable isotope ratios  $\delta D$  ( $^2H/^1H$ ) and  $\delta^{18}O$  ( $^{18}O/^{16}O$ ) of fog water ( $H_2O$ ) (Ingraham and Matthews, 1995). The stable isotopic composition of coastal fog water is typically more enriched in heavier isotopes than that of rain or snow because it is a first-stage condensate off the ocean and forms at low elevation and thus at higher air temperatures (Ingraham and Matthews, 1995; Scholl et al., 2011). Using  $\delta D$  and  $\delta^{18}O$ , Dawson (1998) found that fog drip, on average, represents about 34% of annual hydrologic input to a northern California coastal redwood forests. In a similar study using stable isotopes of fog water and rain as tracers, Ingraham and Matthews (1995) estimate that 25% of groundwater at a coastal site on Point Reyes Peninsula in the Bay Area could be derived from fog-drip recharge.

In addition to studies that quantify fog drip from vegetation, some studies collect and quantify fog water that drips from manmade collectors, known as fog deposition (Goodman, 1985; Ingraham and Matthews, 1988; Ingraham and Matthews, 1995; Schemenauer and Cereceda, 1994; Fischer and Still, 2007; Imteaz et al., 2007, Hiatt et al., 2012). Fischer and Still (2007) suggest that fog deposition from manmade collectors is a reasonable proxy of the fog drip from vegetation. In general, the manmade fog deposition collectors are passive and rely on wind to transport moisture-laden air over a collection surface. However, collectors have incorporated a variety of design elements, which has limited comparative analysis of the controls on fog drip volumes and isotopic

composition across previous studies. Mesh and harp collectors (Fischer and Still, 2007) are the two main design types that have been used in recent research, with the standard fog collector (SFC) (Schemenauer and Cereceda, 1994) being the most commonly used type of mesh collector (Fig. 1). Mesh collectors have vertical and horizontal stands to intercept fog, while harp collectors have only vertical strings. Fog collection rates from mesh and harp collectors are significantly affected by exposure to a fog event, including fog characteristics such as fog duration, type, liquid water content, wind speed, and cross-sectional area of the collector (Ingraham and Matthews, 1998; and Schemenauer and Cereceda, 1991).

The SFC design is highly effective in collecting fog deposition in some environments (Schemenauer and Cereceda, 1991; Imteaz et al., 2011; Hiatt et al., 2012). In El Tofo, Chile, fifty 48 m<sup>2</sup> SFC produced nearly  $7.2 \times 10^3$  liters per day (Schemenauer and Cereceda, 1991), and locally produced 3.86 L/d in Big Sur (Hiatt et al., 2011). The contact points between the collector strands tend to store more water than the filaments used in the harp design. The larger water storage capacity of the mesh collector may increase the lag time between the onset of a fog event and the collection of fog deposition, and thus some mesh collectors may not record input from low-intensity fog events (Fischer and Stills, 2007). During that lag time, evaporation of water on the mesh may allow for fractionation and enrichment of the stable isotope composition of the fog deposition (Fischer and Stills, 2007).

The increased storage and potential for isotopic fractionation of water from the mesh collectors led to the development of the harp collector which consists of two perpendicular harps that intersect at a center post (Fischer and Still, 2007). The harps consist of two layers of monofilament, stretched between two stainless steel rods (Fig. 1). Fog droplets collide with the monofilament and collect in small troughs positioned below the steel rods. While the SFC is most efficient oriented perpendicular to the wind direction, the harp design is less sensitive to changing wind directions. The vertical strings of the harp design retain less residual liquid and minimize post-collection evaporation and isotopic fractionation and better capture low-intensity, short-duration fog events (Fischer and Still, 2007). Surprisingly, no published studies have compared stable isotope composition of fog deposition from co-located SFC and harp collectors.

Furthermore, the lack of large-scale fog collection studies conducted in the Bay Area limit understanding of the conditions that control fog drip in the area. Although some fog deposition studies have been conducted in the Bay Area (Goodman, 1977; Ingraham and Matthews, 1995; Hiatt et al., 2011), no fog deposition models have been developed to understand local conditions or predict fog deposition volume. Imteaz et al. (2011) developed a mathematical model to quantify fog deposition in the Asir region of southwestern Saudi Arabia. The model incorporated the effects of the humidity ratio between air temperature and the dew point, wind velocity, and fog collector area to quantify fog deposition volume. In constructing the model, Imteaz et al. (2011) defined the Fog Potential Index (FPI) term based on the assumption that fog forms when

surrounding air temperature was  $1.0^{\circ}\text{C}$  higher than the corresponding dew point. FPI was used in the model to predict the presences of fog; the higher the FPI value, the greater potential for fog deposition.

While some studies (Fischer and Still, 2007; Imteaz et. al, 2011) that have sought to correlate meteorological conditions to fog deposition volume, relatively few have examined the relationship between meteorological conditions and the isotopic composition of fog deposition. Based on previous work (Schemenauer and Cereceda, 1994; Fischer and Still, 2007), I hypothesize that fog collector design may influence isotopic fractionation of fog water remaining on the collection surface. To test this hypothesis and address the above knowledge gaps, the objective of this thesis is twofold. First, I will use the isotopic values of fog deposition collected by the SFC and harp designs in the same meteorological conditions and during the same fog events to test the hypothesis that collector design affects fractionation and isotopic values of fog deposition. To my knowledge, this is the first study to test fog collector design on stable isotope composition of fog deposition. Second, the meteorological data and fog water collected from the SFC will be used to construct a fog deposition model to compare to other studies using the SFC. From this analysis, I discuss the role of fog as hydrologic input to the Bay Area and implications of ecological demand.

## 2.0 Study Area

Fort Funston, which is part of the Golden Gate National Recreation Area, was selected for the study site because it lies along the southwestern edge of San Francisco

County and is the first location to intercept coastal fog as it moves inland (Fig. 2). The physical processes that dominate the development of marine stratus along the Bay Area coastline during the summer months are the result of anticyclonic circulation of atmospheric and oceanic features originating over the northern Pacific Ocean (Hilliker and Fritsch, 1999; Lebassi et al., 2009). Cool sea-surface temperatures are maintained during summer months as air flows clockwise around a high-pressure system known as the Pacific High that draws both cool air and water southward in the California Current. In addition, alongshore wind stresses drive an upwelling plume, bringing deeper colder water to the surface (Lebassi et al., 2009). Simultaneously, hot temperatures over the continental interior induce a low-pressure area (often referred to as the North American Thermal Low (NATL)). The pressure difference between the Pacific High and the NATL brings an onshore airflow of cool air inland (Lebassi et al., 2009). A temperature inversion develops close to Earth's surface (<200 m) and confines the cool, moisture laden air to low elevations over cool ocean water and promotes vertical mixing that causes thick coastal stratus to develop (Hilliker and Fritsch, 1999).

In addition to the anticyclonic circulation of atmospheric and oceanic features, local geographic features influence the extent and location of inundation and occurrence of maritime fog (Hilliker and Fritsch, 1999). The Santa Cruz Mountains to the south of San Francisco rise between 300–600 m above sea level, whereas the inversion layer boundary fluctuates between 200–400 m. Low elevation gaps in coastal topography, allow marine stratus to infiltrate the Bay Area when the inversion height remains below

the height of the coastal ranges (Hilliker and Fritsch, 1999). The site location is atop a bluff approximately 50 m above sea level and located away from and ocean-side of native vegetation to limit obstruction of fog-laden wind (Fig. 1).

### 3.0 Methods

#### 3.1 Fog Deposition Collectors and Meteorological Instrumentation

A mesh and harp collector were installed at the Fort Funston site (Fig. 1) on June 20, 2012. The mesh collector was built to specifications of the SFC design (Schemenauer and Cereceda, 1994). The SFC design incorporates a double layer of 35% shade coefficient, polypropylene-Raschel mesh, woven into a triangular pattern, and stretched over a 1.0 m<sup>2</sup> metal frame. To maximize collection efficiency, the SFC was oriented perpendicular to the prevailing on-shore wind direction, which is based on long-term data from the San Francisco Public Utilities Commission (SFPUC) (City of San Francisco). The harp collector was built to specifications outlined by Fischer and Still (2007) and installed approximately 1 m north of the SFC (Fig. 1).

To quantify fog deposition, each collector was installed with a Decagon Devices ECRN-100 rain gauge that was positioned beneath the outflow hole of each collection trough (Fig. 1). The rain gauges were modified with a funnel to collect the fog deposition in a sealed Nalgene bottle (Fig. 1). In addition to the two rain gauge beneath each fog collector, a third freestanding rain gauge was installed to record and account for any rainwater precipitation in the SFC or harp collectors. Wind speed, wind direction, relative humidity, and air temperature data were recorded with a Decagon Devices Davis

Cup Anemometer (installed on July 12, 2012) and EHT Humidity and Temperature Sensor. All data was recorded at one-minute intervals with Decagon Devices Em50 Data Loggers. Fog deposition samples and the meteorological data were collected until October 4, 2012.

### 3.2 Isotope Analysis of Fog Deposition

At each site visit, 30 mL fog deposition samples from the sealed Nalgene bottles beneath the SFC and harp were manually collected, filtered through 0.45- $\mu\text{m}$  Envexp filter, and preserved in 30 mL Qorpak glass bottles. Any remaining water from the Nalgene bottles was discarded. Stable isotope ratios  $\delta\text{D}$  ( $^2\text{H}/^1\text{H}$ ) and  $\delta^{18}\text{O}$  ( $^{18}\text{O}/^{16}\text{O}$ ) were measured at California State University East Bay using a Los Gatos Research Liquid-Water Isotope Analyzer spectrometer with precision 0.6‰ and 0.2‰ respectively. The stable isotopic ratios are calibrated using standards based upon the Vienna Standard Meteoric Ocean Water (VSMOW) as a reference to construct a local meteoric water line. The Wilcoxon rank-sum test was used to evaluate if the stable isotope ratios of fog deposition from the SFC were statistically different than stable isotope ratios of fog deposition from the harp collector.

### 3.3 Modeling Fog Deposition Volume

A predictive best-fit linear regression model of fog deposition volume during fog events was developed using fog deposition volumes from the SFC and meteorological data, including fog event duration, relative humidity, temperature, wind speed, wind direction, wind angle deviation from perpendicular, and FPI (Table 7). For deposition

samples that were a mix of two or more fog events, all atmospheric variables recorded during individual events were averaged. Fog deposition volume was estimated from depth measurements recorded by the rain gauge. One tip of the rain gauge is equivalent to 0.2 mm of water per  $\text{m}^2$ , which was estimated to be  $0.4 \times 10^{-2}$  L and was used to calculate total volume of water collected per fog event. Because the presence of fog is difficult to measure with low-cost instruments, a fog event is defined here as the time between the first and final tips of the rain gauge beneath the SFC. Event averages were used to construct a multivariate linear regression model to correlate fog water deposition volume.

### 3.4 Modeling Fog Deposition Isotopes

A predictive best-fit linear regression model of stable isotope ratios of fog deposition during fog events was developed using the stable isotope and meteorological data from the SFC. Relative humidity and air temperature data collected during each fog event were used to calculate the FPI (Imteaz et al., 2011). In addition to FPI, easy to measure meteorological variables, such as event duration, relative humidity, temperature, wind speed, wind direction, and wind angle deviation from perpendicular, were used to construct a multivariate linear regression model to predict stable isotopic values of fog deposition from the SFC where  $\delta^2\text{H}$  (Table 9) and  $\delta^{18}\text{O}$  (Table 10) values for each fog water sample were weighted with inverse variance weighting.

## 4.0 Results

### 4.1 Fog Deposition and Meteorological Data

The SFC recorded a total of 39 fog events during the 68-day collection period (August 1 to October 4, 2012) with a mean event duration of 515 minutes and an event duration maximum of 1,036 minutes (Table 1). The SFC collected a total of 65.2 L and a mean of 1.71 liters per event, while the harp collected a total of 9.53 L and a mean of 0.24 liters per event. No rainfall precipitation was recorded during the collection period. SFC fog deposition occurred most frequently between 20:00 and 23:59, with 20.6 L/m<sup>2</sup> collected, representing 31.7% of the total volume and an hourly deposition maximum of 1.28 L/m<sup>2</sup>, and almost no fog deposition occurred between 11:00 and 17:00 (0.10 L/m<sup>2</sup> collected, and 0.002% of the total volume) (Fig. 3).

The mean and hourly mean maximum wind speed was 4.4 m/s and 8.5 m/s, respectively (Table 2). The mean hourly wind speed increased throughout the morning to approximately 5.0 m/s by 12:00 and remained relatively constant until 20:00 (Fig. 4). The mean and event mean maximum wind speed during fog events was 4.1 m/s and 8.1 m/s (Fig. 5), respectively. The prevailing wind direction ranged from 167° to 247° with a hourly mean of 228° (Fig. 6) and 225° during fog events (Table 3). The wind speed and direction is consistent with previous fog research in the Bay Area (Goodman, 1977).

During the fog events, the mean air temperature ranged from 10.3 to 12.4°C and the maximum air temperature ranged from 10.8 to 14.1 °C (Table 4). The greatest mean

air temperatures were generally between about 10:00 and 20:00 (Fig. 6), which corresponds to the time of day with the least fog deposition (Fig. 3). During the 39 fog events, the mean and maximum FPI ranged from 0.6 to 1.4 and from 0.9 to 1.6, respectively (Table 5). The diel FPI cycle was nearly the inverse of the air temperature, with relatively greater FPI values before 10:00 and after 20:00 and relatively smaller FPI values between 10:00 and 20:00 (Fig. 7). The diel hourly fog deposition cycle was generally consistent with mean hourly FPI, with greater fog deposition and FPI between approximately 19:00 and 12:00 and less fog deposition and FPI between approximately 12:00 and 19:00 (Fig. 8). However, the fluctuations in fog deposition preceded rather than lagged behind similar directional changes in FPI (Fig. 8).

#### 4.2 Isotope Signature of Fog Deposition

From the 39 fog events a total of 30 SFC fog deposition samples had  $\delta^2\text{H}$  and  $\delta^{18}\text{O}$  values within the confidence interval of the LGR Liquid-Water Isotope analyzer (Table 6). The mean  $\delta^2\text{H}$  value was  $-13.74$  with a standard deviation of  $0.80$ , and the mean  $\delta^{18}\text{O}$  value was  $-2.63$  with a standard deviation of  $0.15$ . The relatively lower fog deposition efficiency off the harp collector yielded fog deposition samples with 17  $\delta^2\text{H}$  and 11  $\delta^{18}\text{O}$  values within the confidence interval of the LGR Liquid-Water Isotope analyzer (Table 6). The mean  $\delta^2\text{H}$  value was  $-14.82$  with a standard deviation of  $0.93$ , and the mean  $\delta^{18}\text{O}$  value was  $-2.74$  with a standard deviation of  $0.19$ . The stable isotopic composition of fog deposition samples from the SFC are plotted in Fig. 9. Also shown in Fig. 9 are the global meteoric water (GMW) line (Craig, 1961) and the best-fit regression

line (local meteoric water line) of the fog deposition isotopic values. Most of the fog deposition samples plot below the MWL (Fig. 9).

Using stable isotope values within the confidence interval of the LGR Liquid-Water Isotope analyzer, results of the Wilcoxon rank-sum test ( $\alpha = 0.05$ ) indicate that stable isotope ratios of fog deposition collected from the SFC and harp were not significantly distinguishable for  $\delta^2\text{H}$  ( $p > 0.908$ , 14 sample pairs) or  $\delta^{18}\text{O}$  ( $p > 0.762$ , 10 sample pairs) (Fig. 10a). Results of the Wilcoxon rank-sum test ( $\alpha = 0.05$ ) for all stable isotope values, including those outside the LGR Liquid-Water Isotope analyzer confidence interval, similarly indicate that stable isotope ratios of fog deposition collected from the SFC and harp were not significantly distinguishable for  $\delta^2\text{H}$  ( $p > 0.969$ , 21 sample pairs) or  $\delta^{18}\text{O}$  ( $p > 0.899$ , 21 sample pairs) (Fig. 10b). These results indicate no statistically significant difference in fractionation of stable isotopes between fog deposition collected using the SFC and harp design.

### 4.3 Fog Deposition Volume Model

The best-fit multivariate linear regression model of fog deposition volume ( $R^2 = 0.675$ ) included event duration, relative humidity, air temperature, and wind direction (Table 8). The next best-fit model ( $R^2 = 0.629$ ) included event duration, wind direction, and FPI instead of relative humidity and air temperature. In both models, the most significant explanatory variable was the duration of the fog event ( $p > 0.0001$ ).

#### 4.4 Fog Deposition Isotopic Model

The best-fit multivariate linear regression model of fog deposition  $\delta^2\text{H}$  ( $R^2 = 0.696$ ) and  $\delta^{18}\text{O}$  ( $R^2 = 0.659$ ) values included relative humidity and wind direction (Table 9). In both models the most significant explanatory variable was relative humidity with p values of  $< 0.0001$  and  $0.0005$  for the  $\delta^2\text{H}$  and  $\delta^{18}\text{O}$  models, respectively.

#### 5.0 Discussion

##### 5.1 Fog Deposition and Meteorological Data

During the observation period, the SFC was more efficient than the harp design in collecting larger volumes of fog deposition, even with the apparently larger water storage capacity of the SFC than the harp design. To better understand the role of water storage capacity of the SFC mesh and lag times between the onset of fog and the first fog deposition, the meteorological conditions prior to the first fog deposition should be analyzed. Similarly, the water storage capacity of the SFC mesh may allow fog deposition to occur after the fog dissipates, and thus meteorological conditions during the trailing tail of fog deposition may not necessarily reflect conditions of fog. Thus, the water storage capacity of the SFC mesh and the fog deposition-based definition of fog event effectively omit from the analysis early-stage meteorological conditions and includes meteorological conditions that occurred after the fog dissipated. Defining a fog event using data from an optical fog detector (e.g., Mallant and Kos, 1990) or similar instrumentation would likely improve understanding the controls of the leading and trailing tail of fog deposition.

During periods of no fog and high winds, I observed atmospheric deposition of fine sand on collection surfaces, which required frequent cleaning to remove the sediment. Fine sediment on the collection surfaces may effectively increase the storage capacity of the mesh and collection trough, further increasing the temporal lag between the onset of fog deposition and collection, and may result in under-reporting of the actual fog deposition volume. Also, the sediment periodically clogged the inlet to the rain gauge, effectively delaying or restricting the flow of fog deposition into the rain gauge, thus resulting in under-reporting of the actual fog deposition and (or) possibly enhancing fractionation. Therefore, when the rain gauge was observed to be clogged with sediment, all meteorological data, fog deposition volume, and fog water isotopic concentrations since that last sampling were omitted from the analysis. Although the sediment deposition was not quantified in this study and is unknown, future fog deposition studies would be advised to perform frequent maintenance to limit sediment deposition on collection surfaces.

In addition to sediment deposition, the local wind conditions may have negatively affected collection efficiencies and caused under-reporting of actual fog deposition. The wind speed at Fort Funston (mean ranged from 1.1 to 8.1 m/s (Table 2)) was considerably greater than the mean wind speed (2 to 3 m/s) reported by Fischer and Still (2011). The 50-m bluff west of the Fort Funston study site would likely increase wind speeds as onshore wind is forced upward and over the bluff. The relatively higher wind speeds may have prevented fog deposition from falling in the collections troughs beneath the harp

(1.3-cm wide trough) and SFC (15 cm-wide trough). I frequently observed wet soil directly beneath and downwind of both collectors after fog events, which was likely the result of wind-blown fog deposition from the collectors.

## 5.2 Isotope Geochemistry of Fog Deposition

The harp collector uses vertical monofilaments that retain less water than the SFC mesh and have the design goal of minimizing fractionation and subsequent enrichment of the stable isotopic composition of fog deposition samples (Fischer and Still, 2007). However, results from this study indicate that fog deposition samples collected on the SFC and harp during the same fog events were not significantly distinguishable from one another (Fig. 10), and support the important finding that fractionation of fog deposition is not a function of fog collector design. The advection fog of the Bay Area typically occurs during the night and early morning hours when conditions that limit evaporation are present, including cloud cover, relatively high FPI (high relative humidity), and active fog deposition. Therefore, evaporation and subsequent fractionation are not important processes during fog deposition on either the SFC or harp collector. During the daytime hours when greater air temperature and wind speed favor evaporation, it is likely that any fog deposition remaining on the collection surface is completely evaporated, leaving no imprint on isotopic signature before subsequent fog events.

## 5.3 Fog Deposition Volume Model

The two most statistically significant multivariate linear regression models of fog deposition volume from the SFC include the explanatory variables of event duration,

relative humidity, air temperature, and wind direction (Table 8). In both models, the duration of the fog event is the most statistically significant variable and is directly proportional to fog deposition volume. The wind direction during the fog events was also statistically significant, but inversely proportional to fog deposition volume in both models (Table 8). The SFC was installed so that the mesh surface was oriented perpendicular ( $302^\circ$ ) to the prevailing on-shore wind direction. The average wind directions during fog events ranged from  $167^\circ$  to  $247^\circ$  (Table 4), with deviations from perpendicular ranging between  $0^\circ$  to  $45^\circ$ . Wind direction deviations from perpendicular had less of an effect on fog deposition volume than suggested by previous studies (Fischer and Still, 2007).

In addition to fog event duration and wind direction, the relative humidity and air temperature were statistically significant in Model A ( $R^2 = 0.675$ ) (Table 8) and FPI was statistically significant in Model B ( $R^2 = 0.629$ ) (Table 8). Relative humidity and temperature had a stronger correlation with fog water deposition volume than FPI, which is dependent on the difference between dew point and air temperature (Imteaz et al., 2011). The predictive fog volume model proposed by Imteaz et al. (2011) uses FPI values generally greater than those calculated in this study. The higher FPI values are likely attributed to advection of clouds over higher terrain tend to have larger fog droplet diameter and higher liquid water content, and fog water collection volume water contents than fog produced at the sea surface (Goodman, 1977; Schemenauer and Cereceda, 1991), and due to the differences in the site characterization between these two studies.

Drawing direct comparisons between the two sites is difficult. The study sites reported by Imteaz et al. (2011) were located atop a coastal mountain chain, with heights approximately 2200 m, along the western shore of the Red Sea. The sea surface temperatures of the Red Sea region are substantially higher at sea level, varying annually between 22°-33° (UNEP, 1997), whereas sea surface temperatures for San Francisco range 11°C-16°C (NOAA). The total amount of water vapor held by the air would be higher for this location. The temperatures recorded at collection sites are colder than those at Fort Funston, and the total amount of condensable water collected at 2200 m would be greater than water volume expected in this study. Fog droplet diameter, liquid water content, and fog water collection volume have been shown to be positively correlated with elevation (Goodman, 1977; Fischer and Still, 2007).

#### 5.4 Fog Deposition Isotope Model

The two most statistically significant multivariate linear regression models of fog deposition isotope values ( $\delta^2\text{H}$  and  $\delta^{18}\text{O}$ ) from the SFC include the explanatory variables relative humidity and wind direction. Interestingly, air temperature was a poor proxy in previous model simulations and poorly correlated to isotopic composition even though air temperature and isotopic fractionation have a strong linear relationship (Dansgaard, 1964). In both the  $\delta^2\text{H}$  and  $\delta^{18}\text{O}$  models, relative humidity was most strongly correlated to isotopic compositions with p-values < 0.0001 and 0.0005, respectively (Table 9). For the 19 fog samples used to constrain these models, average relative humidity values ranged between 0.95 and 0.97. Similar to models for fog deposition volume, wind

direction was also a statistically significant explanatory variable for the isotope models. Wind direction strongly links vapor source region to fog deposition isotopic composition, and as water evaporates off of a colder ocean surface the water vapor experiences greater isotopic depletion than water derived from a warmer source (Craig, 1961). Wind direction strongly correlates with deuterium-excess (d-excess), which is correlated with the physical conditions of the oceanic source area of the precipitation (Dansgaard, 1964; Froehlich et al., 2002). Wind direction is the strongest indicator because it provides information about the isotopic signature of the vapor, more so than meteorological conditions present at the time of deposition. Lower d-excess values, characterized by increased evaporation in warmer air temperatures, suggest a less northerly vapor source (Figure 11).

## 6.0 Conclusions

The first objective of this investigation was to compare the isotopic values of fog deposition from SFC and harp collectors in the same meteorological conditions during the same fog event. Results of this study indicate that the values of  $\delta^2\text{H}$  and  $\delta^{18}\text{O}$  for fog deposition during the same event were not significantly distinguishable for samples from the SFC and harp collectors. These results support the important finding that the differences in design of the mesh and harp collectors does not significantly affect the isotopic fractionation of fog deposition collected from the advection fog in the Bay Area. These findings indicate that either the SFC or harp could be used to collect fog deposition for analysis of stable isotopes that represents fog drip in coastal areas of California.

The second objective was to expand on previous studies to construct models to correlate meteorological variables with fog water deposition volume and isotopic composition. Model outputs strongly correlate fog deposition volume with event duration, relative humidity, temperature, and wind direction, without respect to angle efficiency or mesh panel orientation. Similarly, relative humidity and wind direction were the most strongly correlated meteorological variables in constraining models of isotopic composition. Previous work used to develop a FPI did not significantly improve model output in the Bay Area meteorological conditions. Moreover, an important finding from this study is that easily obtained meteorological data can serve as a proxy for fog water deposition volume and isotopic composition. With relatively low-cost meteorological instruments, future fog drip and deposition studies in the Bay Area are encouraged to collect wind direction data because it is strongly correlated to collect fog deposition volumes and isotopic composition.

## 7.0 References

- Azevedo, J., and Morgan, D. L. (1974) Fog precipitation in coastal California forests. *Ecology* 55 (5), 1135-1141.
- Burgess, S.S.O, and Dawson, T.E. (2004) The contribution of fog to the water relations of *Sequoia sempervirens* (D. Don): foliar uptake and prevention of dehydration. *Plant Cell and Environment* 27(8): 1023-1034.
- Byers, H. R. (1953) Coast redwoods and fog drip. *Ecology* 34 (1), 192.
- City of San Francisco. San Francisco Wind Monitoring Data – Current. [online] Available from: <https://data.sfgov.org/Environmental-and-Conservation/San-Francisco-Wind-Monitoring-Data-Current/bkgs-xaqe> (Accessed 13 May, 2014).
- Clark, I. D., and Fritz, P. (1997) Environmental isotopes in hydrogeology. Boca Raton: CRC Press. Lewis Publishers.
- Craig, H. (1961), Isotopic variations in meteoric waters, *Science*, 133, 1702-1703.
- Dansgaard, W. (1964) Stable isotopes in precipitation. *Tellus* 16 (4), 436-468.
- Dawson, T. E. (1998) Fog in the California redwood forest: ecosystem inputs and use by plants. *Oecologia* 117 (4), 476-485.
- Fischer, D. T., and Still, C. J. (2007) Evaluating patterns of fog water deposition and isotopic composition of the California Channel Islands. *Water Resources Research* 43, doi: 10.1029/2006WR005124.
- Froehlich, K., Gibson, J.J., and Aggarwal, P. (2002) Deuterium excess in precipitation and its climatological significance. Study of environmental change using isotope techniques, C&S Paper Series 13/P, pp. 54-65, International Atomic Energy Agency, Vienna, Austria, ISBN 92-0-116402-5.
- Goodman, J. (1977) The microstructure of California coastal fog and stratus. *Journal of Applied Meteorology* 16, 1056-1067.
- Goodman, J. (1985) The collection of fog drip. *Water Resources Research* 21 (3), 392-394.

- Hiatt, C., Fernandez, D., and Potter, C. (2012) Measurements of fog water deposition on the California Central Coast. *Atmospheric and Climate Sciences* (2), 525-531.
- Hilliker, J. L., and Fritsch, J. M. (1999) An observation-based statistical system for warm-season hourly probabilistic forecasts of low ceiling at the San Francisco International airport. *Journal of Applied Meteorology* 38, 1692-1705.
- Imteaz, M. A., Al-hassan, G., Shanableh, A., and Naser, J. (2011) Development of a mathematical model for the quantification of fog-collection. *Resources, Conservation and Recycling* 57, 10-14.
- Ingraham, N. L. and Matthews, R. A. (1995) The importance of fog-drip water to vegetation: Point Reyes Peninsula, California. *Journal of Hydrology* 164 (1-4), 269-285.
- Ingraham, N. L., and Matthews, R. A. (1998) Fog drip as a source of groundwater recharge in northern Kenya. *Water Resources Research* 24, 1406-1410.
- Lebassi, B., Gonzalez, J., Drazen, F., Maurer, E., Miller, N., Milesi, C., Switzer, P., and Bornstein, R. (2009) Observed 1970-2005 cooling of summer daytime temperatures in coastal California. *Journal of Climate* 22, 3558-3573.
- Mallant, R.K.A.M., and Kos, G.P.A. (1990) An optical devise for the detection of clouds and fog, *Aerosol Science and Technology* 13: 196-2002.
- Means, T. H. (1927) Fog precipitated by trees. *Science* 66 (1713), 402-403.
- NOAA. National Oceanic and Atmospheric Administration – National Oceanographic Data Center. Water temperature table of the central Pacific coast. [online] Available from: [www.nodc.noaa.gov/dsdt/cwtg/cpac.html](http://www.nodc.noaa.gov/dsdt/cwtg/cpac.html) (Accessed 14 May, 2014).
- Oberlander, G.T. (1956) Summer fog precipitation on the San Francisco Peninsula. *Ecology* 37 (4), 851.
- Schemenauer, R. S., and Cereceda, P. (1991) Fog-water collection in arid coastal locations, *Ambio* 20, 303-308.
- Schemenauer, R. S., and Cereceda, P. (1994) A proposed standard fog collector for use in high-elevation regions. *Journal of Applied Meteorology* 33, 1313-1322.

Scholl, M., Eugster, W., and Burkard, R. (2011) Understanding the role of fog in forest hydrology: stable isotopes as tools for determining input and partitioning of cloud water in montane forests. *Hydrological Processes* 25 (3), 353-366.

UNEP, 1997. Assessment of Land-Based Sources and Activities Affecting the Marine Environment in the Red Sea and Gulf of Aden. UNEP Regional Seas Report and Studies, No. 166. United Nations Environment Programme.

## FIGURES

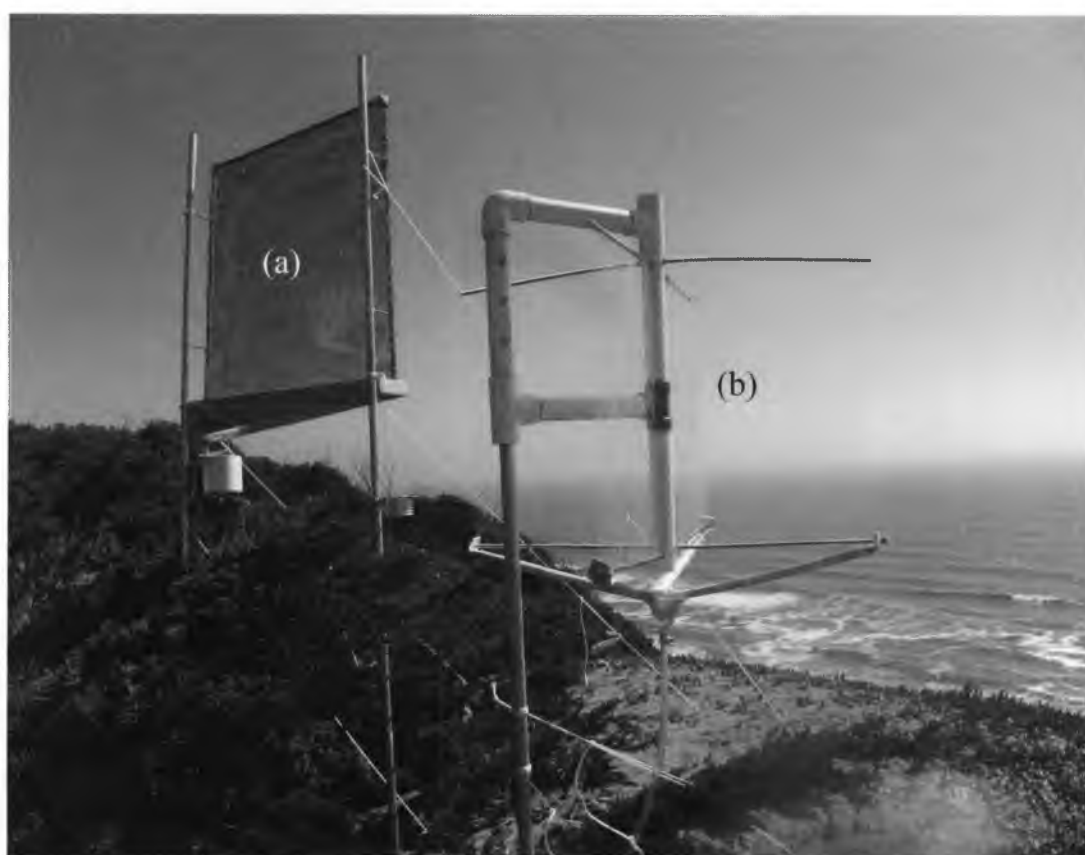


Figure 1. Collection site at Fort Funston installed with a standard fog collector (SFC) (a) (Schemenauer and Cerceda, 1994) and a harp collector (b) (Fischer and Still, 2007). Each collector was modified with a tipping bucket rain gauge to quantify fog deposition that dripped from the collector surface. A funnel positioned below the rain gauges was attached to a closed Nalgene bottle from which fog water samples were collected for isotopic analysis. Additional instrumentation at the site recorded wind speed, wind direction, temperature, and relative humidity data at one-minute intervals.



Figure 2. Location of the study area in Fort Funston National Park, California. Instrumentation was installed atop the bluff on the western edge of the Fort Funston, north of Battery Davis.

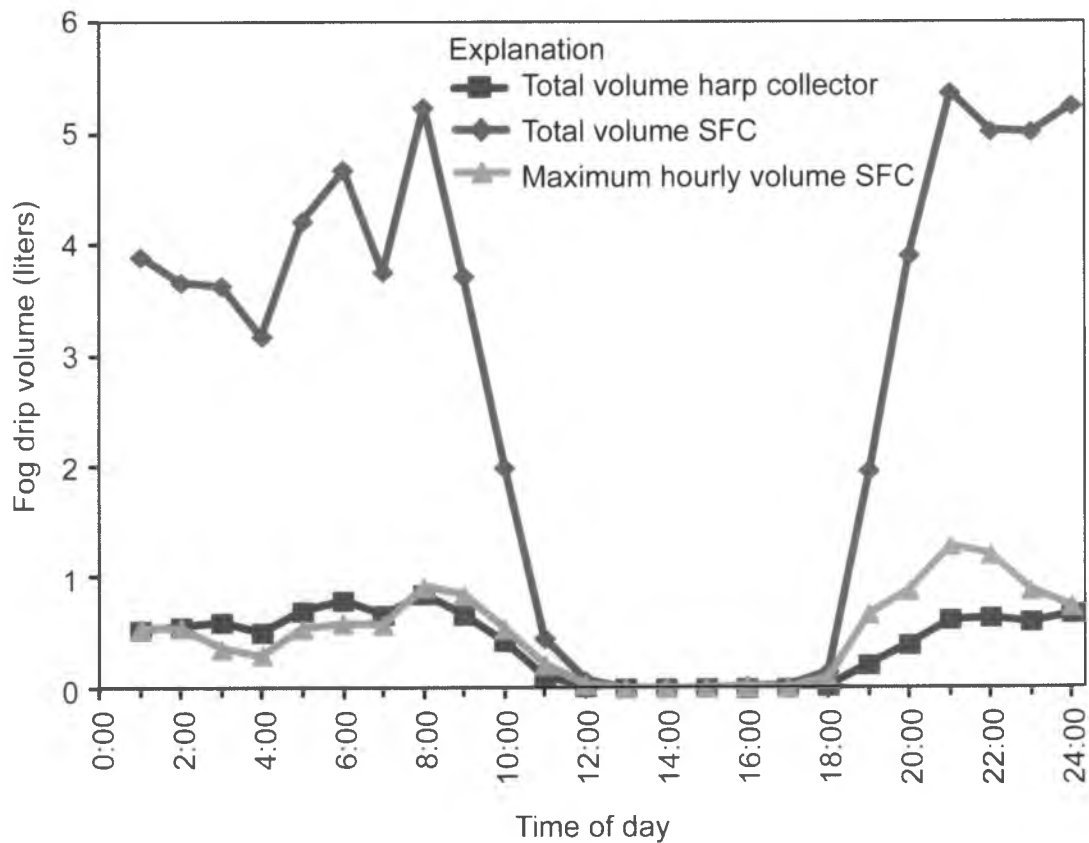


Fig. 3: Fog deposition volume by the standard fog collector (SFC) and harp collector during the 2012 observation period.

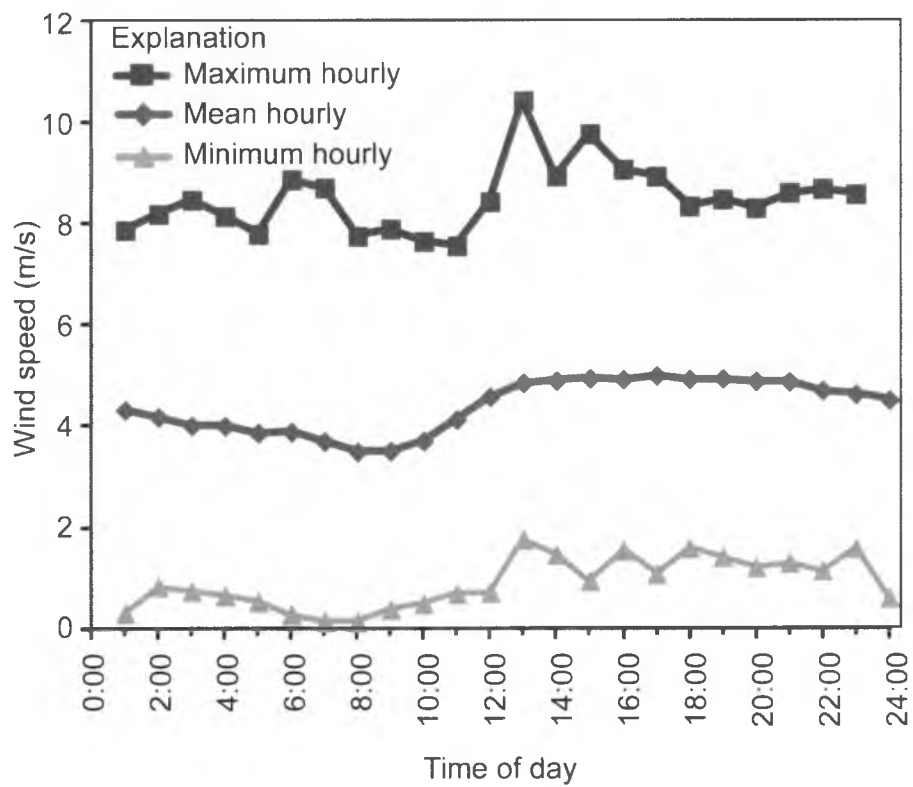


Figure 4. Mean hourly wind speed during the 2012 observation period.

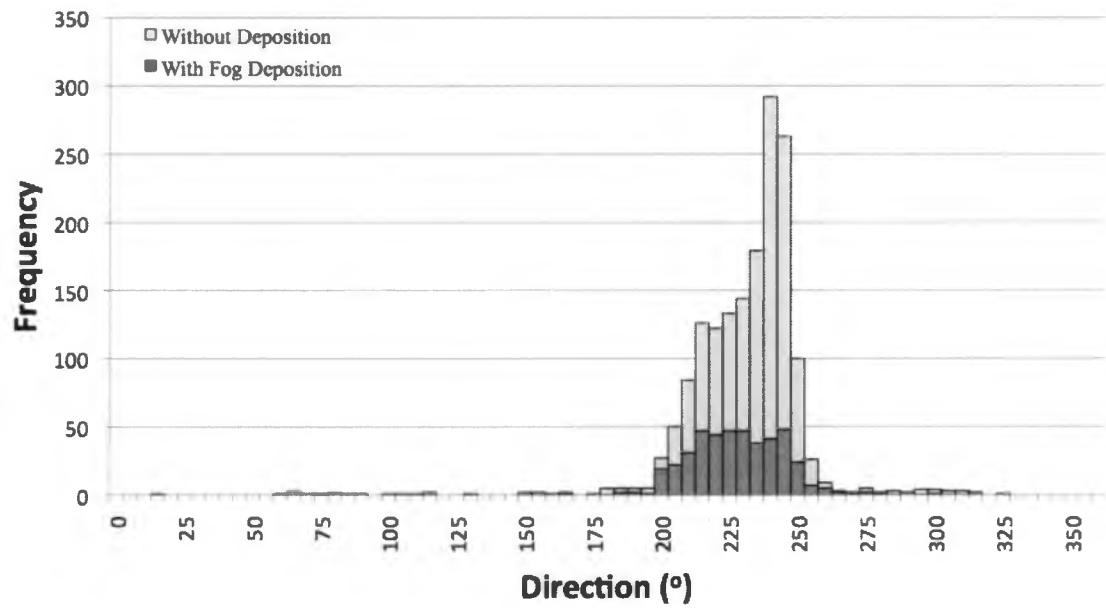


Fig. 5: Histogram of hourly average wind direction during the 2012 observational period. The shaded boxes represent hourly average wind directions for hours, which fog deposition was recorded by the SFC.

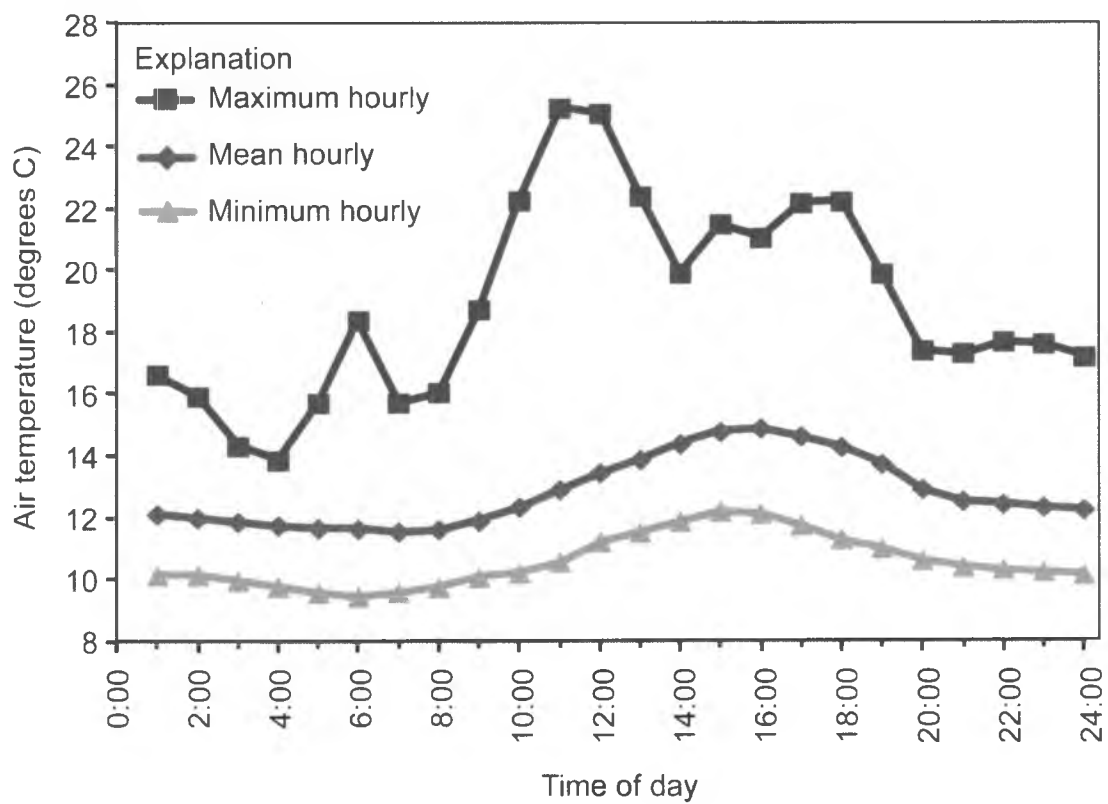


Fig. 6: Hourly air temperature during the 2012 observational period.

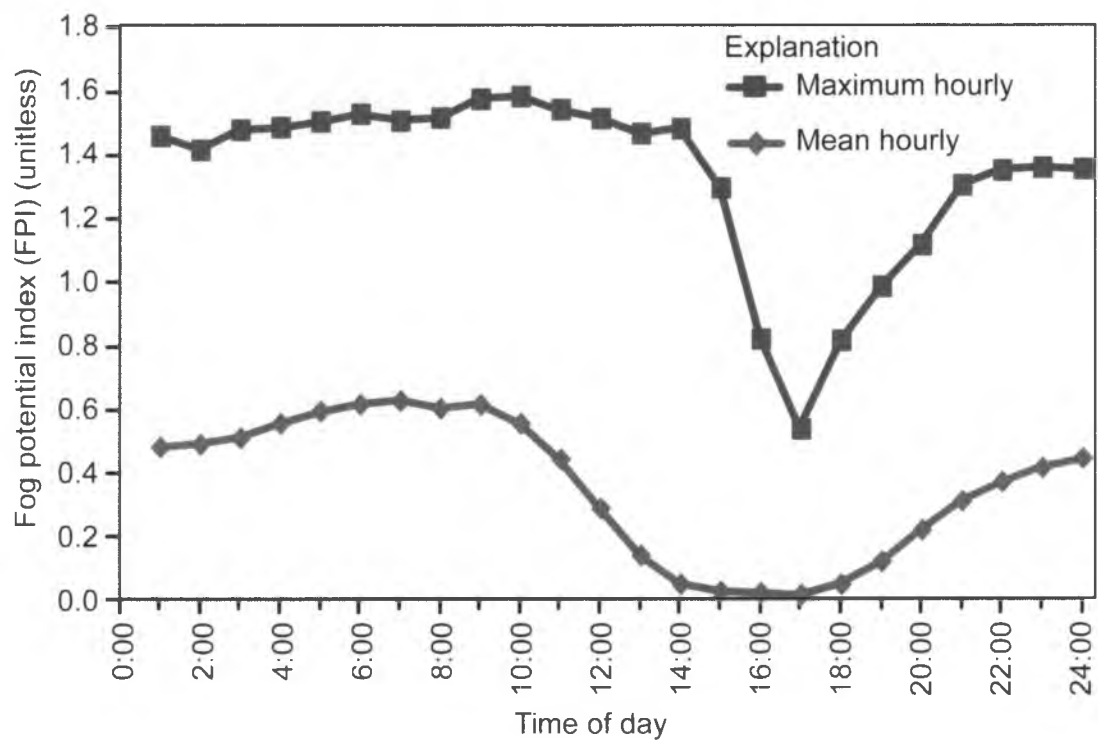


Figure 7. Hourly fog potential index (FPI) during the 2102 observation period.

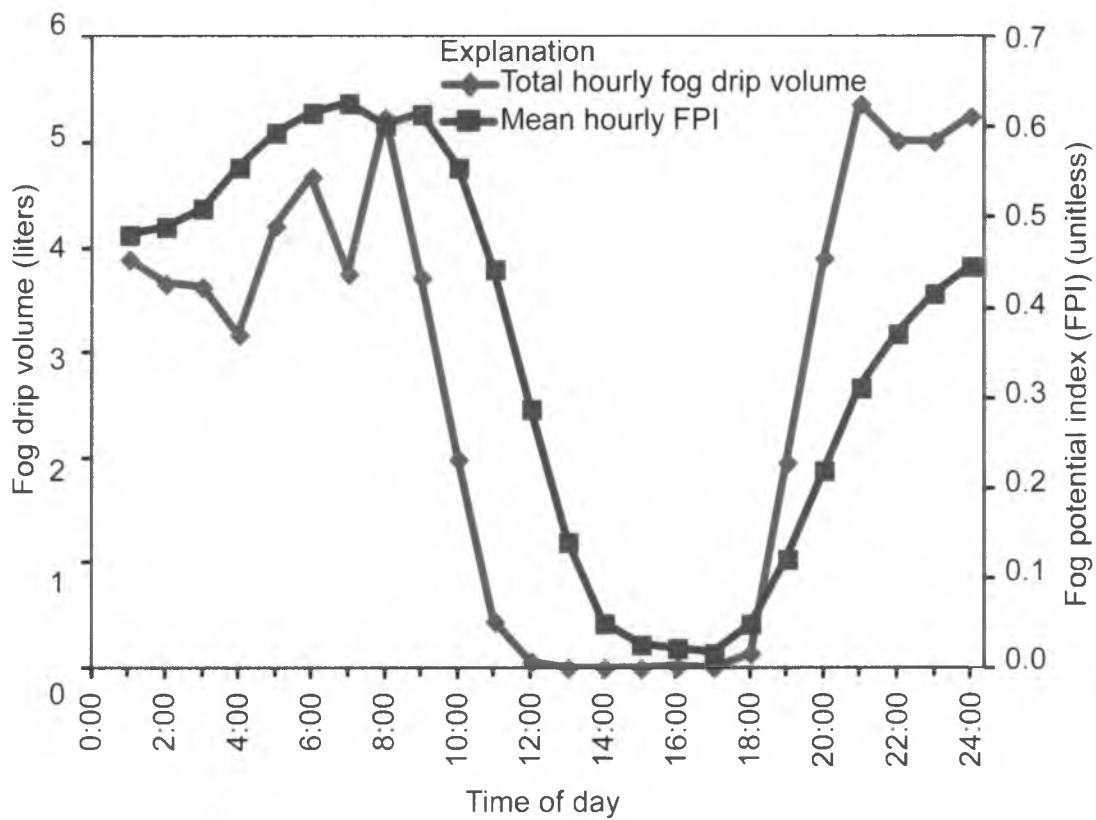


Fig. 8: Total hourly fog deposition volume and mean hourly fog potential index (FPI) during the 2012 observational period.



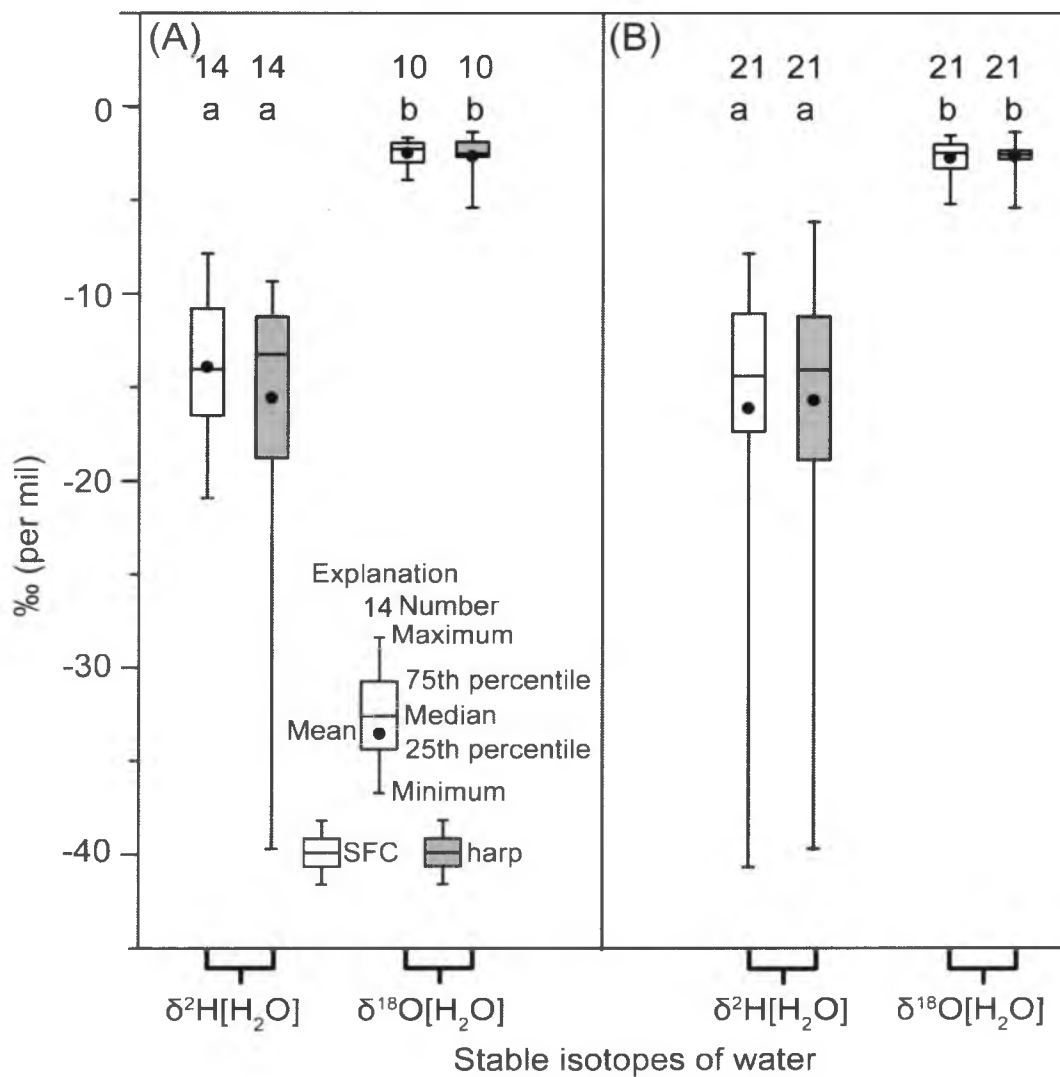


Figure 10. Boxplot of  $\delta^2\text{H}[\text{H}_2\text{O}]$  and  $\delta^{18}\text{O}[\text{H}_2\text{O}]$  from fog drip at the standard fog collector (SFC) and harp collector for samples (A) within and (B) outside the confidence interval of the LGR Liquid-Water Isotope analyzer. Boxplots with different letters have significantly different median values at alpha ( $\alpha$ ) = 0.05 (Kruskal-Wallis and Steel-Dwass tests).

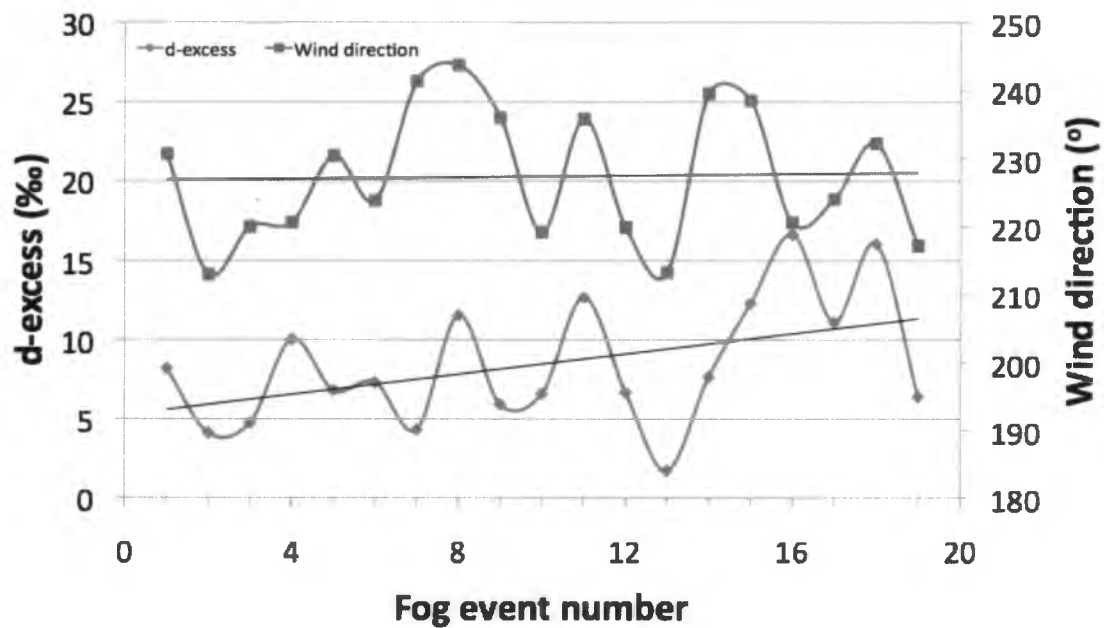


Figure 11. Deuterium excess of fog water samples and mean wind direction data for fog events during the 2012 observational period. Also shown are the best-fit regression lines of the data.

## TABLES

Table 1. Fog event duration, total fog deposition volume, and calculated fog deposition rates (min; L; and L/hr) for fog events monitored by the SFC (Schemenauer and Cerceda, 1994) at Fort Funston between August 1, 2012 and October 4, 2012. The length of a fog event was defined as the time interval between the first and last recorded tips of the rain gauge to during one consecutive series.

Event Number	Collection Date	Duration (min)	Average Relative Humidity	Fog Deposition Volume (L)	Rate of deposition (L/hr)
1	8/1/12	504	0.95	1.78	0.21
2	8/1/12	603	0.96	1.98	0.20
3	8/1/12	523	0.96	0.56	0.06
4	8/1/12	37	0.96	0.02	0.03
5	8/1/12	198	0.94	0.22	0.07
6	8/2/12	658	0.95	0.64	0.06
7	8/3/12	700	0.96	1.36	0.12
8	8/6/12	527	0.96	0.64	0.07
9	8/6/12	1,033	0.97	9.51	0.55
10	8/13/12	173	0.95	0.15	0.05
11	8/13/12	107	0.95	0.22	0.12
12	8/13/12	692	0.96	1.94	0.17
13	8/13/12	677	0.96	0.99	0.09
14	8/13/12	676	0.96	1.70	0.15
15	8/14/12	732	0.97	3.38	0.28
16	8/20/12	730	0.96	0.95	0.08
17	8/20/12	556	0.97	1.03	0.11
18	8/21/12	389	0.97	0.83	0.13
19	8/22/12	496	0.97	1.20	0.14
20	8/23/12	211	0.96	0.10	0.03
21	8/23/12	92	0.96	0.07	0.04
22	8/25/12	138	0.96	1.27	0.55
23	8/25/12	165	0.96	0.22	0.08
24	8/31/12	70	0.95	0.03	0.02
25	8/31/12	289	0.95	0.17	0.03
26	8/31/12	373	0.95	0.42	0.07
27	8/31/12	288	0.95	0.54	0.11
28	9/05/12	799	0.96	1.86	0.14
29	9/05/12	532	0.96	2.74	0.31
30	9/05/12	422	0.97	3.64	0.52
31	9/05/12	843	0.97	4.85	0.35
32	9/13/12	626	0.96	1.18	0.11
33	9/17/12	325	0.96	0.47	0.09
34	9/25/12	899	0.96	3.18	0.21
35	9/25/12	335	0.97	2.24	0.40
36	9/25/12	945	0.97	3.66	0.23

Table 1. Fog event duration, total fog deposition volume, and calculated fog deposition rates (min; L; and L/hr) for fog events monitored by the SFC (Schemenauer and Cerceda, 1994) at Fort Funston between August 1, 2012 and October 4, 2012. The length of a fog event was defined as the time interval between the first and last recorded tips of the rain gauge to during one consecutive series—Continued.

Event Number	Collection Date	Duration (min)	Average Relative Humidity	Fog Deposition Volume (L)	Rate of deposition (L/hr)
37	9/27/12	852	0.97	2.49	0.18
38	9/28/12	1036	0.97	5.28	0.31
39	10/4/12	840	0.97	3.26	0.23

Table 2. Summary statistics of wind speed collected at Fort Funston between August 1, 2012 and October 4, 2012 (m/s).

Wind Speed (m/s)						
Fog Event Statistics						
Event Number	Minimum	Median	Maximum	Average	Sample Average	Collection Date
1	2.1	4.9	8.7	5.0		
2	2.0	5.3	7.3	5.3		
3	1.8	3.8	5.9	3.9		
4	1.2	2.0	3.2	2.0		
5	5.9	8.0	10.5	8.1	5.0	8/1/12
6	3.4	6.2	9.0	6.1	6.1	8/2/12
7	3.9	6.5	9.1	6.5	6.5	8/3/12
8	1.9	6.4	10.2	6.3		
9	2.0	3.9	7.6	4.1	4.9	8/6/12
10	1.0	2.4	5.1	2.8		
11	2.4	4.4	6.3	4.4		
12	1.9	4.7	7.0	4.7		
13	1.2	3.8	6.6	3.9		
14	0.6	2.4	4.6	2.5	3.7	8/13/12
15	2.0	4.6	6.6	4.5	4.5	8/14/12
16	1.9	4.3	8.2	4.5		
17	1.0	3.5	6.1	3.5	4.1	8/20/12
18	2.0	4.2	7.4	4.3	4.3	8/21/12
19	0.9	4.7	8.5	4.7	4.7	8/22/12
20	2.4	4.8	6.9	4.6		
21	2.4	5.0	6.8	5.0	4.8	8/23/12
22	4.0	6.9	9.1	6.8		
23	1.9	4.4	7.7	4.4	5.5	8/25/12
24	0.2	1.0	2.1	1.1		
25	1.7	3.5	5.2	3.6		
26	3.5	5.7	7.7	5.7		
27	2.2	4.4	8.5	4.6	4.5	8/31/12
28	0.0	1.7	4.1	1.8		
29	1.5	3.0	5.1	3.1		
30	0.9	3.8	5.8	3.6		
31	0.8	4.3	6.7	4.3	3.2	9/5/12
32	0.1	1.6	3.6	1.6	1.6	9/13/12
33	0.9	2.4	4.0	2.4	2.4	9/17/12
34	0.0	2.4	6.8	2.5		
35	2.9	6.3	8.4	6.3		
36	0.0	3.7	7.2	3.5	3.5	9/25/12
37	0.2	2.7	5.9	2.7	2.7	9/27/12
38	0.3	4.5	7.4	4.2	4.2	9/28/12
39	0.0	2.2	4.9	2.1	2.1	10/4/12

Table 3. Summary statistics of wind direction Collected at Fort Funston between August 1, 2012 and October 4, 2012.

Wind direction						
Fog Event Statistics						
Event Number	Minimum	Median	Maximum	Average	Sample Average	Collection Date
1	97	330	339	224		
2	150	220	329	223		
3	1	220	329	223		
4	118	164	217	167		
5	182	214	284	216	231	8/1/12
6	141	213	289	213	213	8/2/12
7	162	218	318	220	220	8/3/12
8	188	228	233	232		
9	186	213	265	215	221	8/6/12
10	51	237	328	237		
11	192	226	315	231		
12	159	216	316	217		
13	115	232	336	235		
14	4	235	341	238	230	8/13/12
15	163	221	350	224	224	8/14/12
16	51	239	327	241		
17	159	240	338	242	241	8/20/12
18	156	241	329	244	244	8/21/12
19	201	232	340	236	236	8/22/12
20	191	221	297	223		
21	188	210	252	211	219	8/23/12
22	184	221	292	223		
23	166	244	343	247	236	8/25/12
24	220	233	245	233		
25	148	206	248	203		
26	161	216	294	216		
27	185	235	328	239	220	8/31/12
28	164	209	328	214		
29	142	204	271	204		
30	141	206	262	204		
31	129	220	328	223	213	9/5/12
32	107	238	346	240	240	9/13/12
33	123	235	329	239	239	9/17/12
34	34	220	355	234		
35	153	209	278	210		
36	14	211	328	212	221	9/25/12
37	147	222	319	224	224	9/27/12
38	181	228	328	232	232	9/28/12
39	8	229	328	217	217	10/4/12

Table 4. Summary statistics of air temperature at Fort Funston between August 1, 2012 and October 4, 2012.

Temperature (°C)						
Fog Event Statistics						
Event Number	Minimum	Median	Maximum	Average	Sample Average	Collection Date
1	10.7	12.0	12.4	11.8		
2	11.2	11.7	12.2	11.7		
3	11.1	11.5	11.9	11.5		
4	11.3	11.5	11.7	11.5		
5	11.1	11.4	11.8	11.5	11.7	8/1/12
6	10.8	11.5	12.1	11.5	11.5	8/2/12
7	10.9	11.3	11.5	11.2	11.2	8/3/12
8	10.5	11.0	11.5	11.0		
9	12.6	13.0	14.0	13.1	12.4	8/6/12
10	11.1	11.4	11.8	11.4		
11	10.4	10.8	11.2	10.8		
12	10.3	10.9	11.3	11.8		
13	10.1	10.8	11.1	10.7		
14	10.0	10.8	11.5	10.8	10.8	8/13/12
15	10.9	11.2	12.5	11.3	11.3	8/14/12
16	10.9	11.4	12.0	11.4		
17	10.4	10.7	11.1	10.7	11.1	8/20/12
18	10.9	11.3	11.6	11.2	11.2	8/21/12
19	10.7	11.1	11.6	11.1	11.1	8/22/12
20	12.3	12.5	12.8	12.6		
21	12.1	12.2	12.3	12.2	12.4	8/23/12
22	10.3	10.7	11.2	10.7		
23	10.7	10.9	11.2	10.9	10.8	8/25/12
24	13.5	13.6	13.8	13.6		
25	11.6	11.9	12.1	11.9		
26	11.2	11.6	12.1	11.7		
27	12.0	12.4	12.7	12.3	12.0	8/31/12
28	10.0	10.9	11.4	10.8		
29	10.4	11.3	11.6	11.1		
30	9.7	10.2	11.5	10.4		
31	9.9	10.3	11.7	10.4	10.7	9/5/12
32	10.8	11.2	12.3	11.3	11.3	9/13/12
33	10.1	10.4	10.8	10.4	10.4	9/17/12
34	9.3	10.2	11.2	10.2		
35	11.0	11.3	11.6	11.3		
36	10.1	11.1	11.2	10.2	10.7	9/25/12
37	9.8	10.3	10.9	10.3	10.3	9/27/12
38	9.6	11.1	12.3	10.9	10.9	9/28/12
39	9.6	10.4	11.4	10.4	10.4	10/4/12

Table 5. Summary statistics of Fog Potential Index (FPI) (Imteaz et al., 2011) calculated from temperature and relative humidity data collected at Fort Funston between August 1, 2012 and October 4, 2012.

Fog Potential Index (FPI)						
Fog Event Statistics						
Event Number	Minimum	Median	Maximum	Average	Sample Average	Collection Date
1	0.0	0.6	0.8	0.6		
2	0.6	0.9	1.2	0.9		
3	0.6	0.8	1.0	0.8		
4	0.8	0.8	0.8	0.8		
5	0.0	0.3	0.6	0.3		
6	0.0	0.8	1.1	0.6	0.7	8/1/12
7	0.7	1.1	1.1	1.0	0.6	8/2/12
8	0.7	0.8	1.1	0.9	1.0	8/3/12
9	1.0	1.3	1.5	1.3	1.1	8/6/12
10	0.3	0.5	0.6	0.5		
11	0.5	0.6	0.8	0.6	1.0	8/13/12
12	0.5	1.1	1.3	1.1		
13	0.6	1.1	1.3	1.1		
14	0.8	1.1	1.3	1.1		
15	0.8	1.2	1.5	1.2		
16	0.9	1.2	1.4	1.2	1.2	8/20/12
17	1.0	1.3	1.3	1.2		
18	1.1	1.3	1.4	1.2	1.2	8/21/12
19	0.0	1.1	1.4	0.9	0.9	8/22/12
20	0.9	1.2	1.2	1.2	1.2	8/23/12
21	1.2	1.2	1.2	1.2		
22	0.7	1.2	1.3	1.1	1.0	8/25/12
23	0.7	0.9	1.1	0.9		
24	0.6	0.8	0.8	0.7	0.7	8/31/12
25	0.0	0.6	0.6	0.5		
26	0.5	0.6	0.9	0.7		
27	0.5	0.7	0.9	0.8		
28	0.5	1.0	1.3	0.9		
29	0.5	1.2	1.4	1.2	1.2	9/5/12
30	1.2	1.3	1.5	1.3		
31	1.0	1.5	1.6	1.4		
32	0.9	1.1	1.3	1.1	1.1	9/13/12
33	0.6	1.0	1.1	0.9	0.9	9/17/12
34	0.1	1.1	1.3	1.0	1.2	9/25/12
35	1.0	1.3	1.4	1.3		
36	1.0	1.3	1.4	1.2		
37	0.4	1.3	1.4	1.2	1.2	9/25/12
37	0.7	1.2	1.5	1.3	1.3	9/27/12
38	1.1	1.5	1.6	1.4	1.4	9/28/12
39	0.8	1.4	1.6	1.4	1.4	10/4/12

Table 6. Stable isotope data collected at Fort Funston between August 1, 2012 and October 4, 2012. Fog water samples were run for stable isotopes of  $^{18}\text{O}$  and deuterium on a LGR Isotope Analyzer at University of California East Bay. Fog water samples were collected on a Standard Fog Collector (SFC) (Schemenauer and Cerceda, 1994) and a harp collector (Fischer and Still, 2007). Isotopic values listed in italics were outside of the LGR confidence interval of 0.2‰ for  $^{18}\text{O}$ , and 0.6‰ for deuterium.

Sample Collection		Fog Collector							
Sample Date	Time	SFC				Harp			
		$\delta\text{D}$	std	$\delta^{18}\text{O}$	std	$\delta\text{D}$	std	$\delta^{18}\text{O}$	std
6/22/12		-40.67	8.24	-5.20	0.79	-6.18	0.65	-2.45	0.37
6/24/12		-13.14	3.86	-3.35	0.28				
6/28/12		-24.29	0.41	-3.25	0.05				
6/29/12		-20.54	1.83	-2.50	0.21	-20.79	2.20	-2.80	0.64
6/30/12		-13.13	0.68	-1.55	0.23	-13.21	0.96	-3.31	0.53
7/7/12		-13.11	0.66	-2.46	0.04				
7/8/12		-16.65	1.28	-3.56	0.15	-39.68	1.12	-5.40	0.23
7/9/12		-20.16	0.54	-3.91	0.17	-20.36	0.93	-3.67	0.29
7/10/12	15:30	-14.64	0.18	-3.30	0.14	-22.88	10.63	-2.87	0.83
7/11/12	16:45	-11.07	1.95	-1.57	0.38	-14.26	3.29	-2.56	0.64
7/12/12	13:00	-7.85	1.09	-2.02	0.09	-11.23	1.33	-1.88	0.20
7/13/12	16:15	-29.69	9.22	-3.50	0.55				
7/14/12	14:45	-16.52	0.48	-2.97	0.19	-9.35	1.14	-2.24	0.45
7/17/12	16:35	-14.38	0.83	-2.48	0.08	-18.85	0.86	-2.36	0.24
7/26/12	15:15	-30.30	7.16	-4.81	0.40	-17.85	0.82	-3.28	0.12
8/1/12	13:10	-20.91	0.56	-3.51	0.11	-18.77	1.49	-2.56	0.32
8/2/12		-19.30	0.94	-2.77	0.21				
8/3/12	16:45	-16.23	1.28	-2.15	0.19	-14.07	0.59	-2.63	0.38
8/6/12	16:45	-17.36	10.62	-3.16	0.78	-19.99	9.60	-2.46	0.73
8/13/12		-9.08	1.19	-1.95	0.04	-9.37	1.21	-2.53	0.13
8/14/12	19:45	-8.91	0.56	-1.68	0.15	-9.66	0.80	-1.36	0.27
8/17/12	16:45	-10.80	0.43	-1.90	0.05	-12.24	1.34	-2.12	0.09
8/20/12	20:35	-14.40	1.09	-2.44	0.14	-11.69	0.43	-2.54	0.29
8/21/12	17:20	-9.01	0.32	-2.33	0.20	-10.00	1.80	-1.98	0.38
8/22/12	17:35	-12.24	1.34	-2.12	0.09	-13.29	0.35	-1.90	0.10
8/23/12	17:00	-19.38	7.81	-2.64	0.63				
8/25/12	15:55	-6.90	0.97	-2.74	0.19				
8/31/12	17:00	-13.69	0.93	-2.50	0.16	-15.93	0.85	-2.68	0.10
9/5/12	18:05	-17.10	0.30	-2.14	0.28				
9/13/12	16:25	-20.19	0.54	-3.60	0.26				
9/17/12	18:00	-17.03	0.82	-3.31	0.20				
9/25/12	14:12	-11.08	0.66	-2.22	0.16				
9/27/12	12:50	-9.48	0.68	-3.11	0.13				
9/28/12	18:10	-12.74	1.05	-3.01	0.27				
10/4/12	17:40	-7.72	0.48	-2.99	0.11				

Table 7. Summary of explanatory variables for fog deposition model.

<b>Term</b>	<b>R2</b>	<b>Estimate</b>	<b>p-value</b>
Duration	0.534	0.005	<0.0001
Relative humidity	0.307	132.4	0.0003
Temperature	0.005	-0.183	0.6607
Wind speed	0.008	-0.110	0.5810
Wind direction	0.020	-0.017	0.3893
Wind deviation	0.057	-0.047	0.1428
FPI	0.344	3.912	<0.0001

Table 8. Multivariate linear regression model outputs for fog deposition volume.

<b>Model A</b>			
<b>R<sup>2</sup></b>	<b>Term</b>	<b>Estimate</b>	<b>p value</b>
0.675	Intercept	-74.51	0.0143
	Duration	0.004	<0.0001
	Relative Humidity	74.32	0.0141
	Temperature	0.673	0.0199
	Wind direction	-0.022	0.0678
<b>Model B</b>			
<b>R<sup>2</sup></b>	<b>Term</b>	<b>Estimate</b>	<b>p value</b>
0.629	Intercept	3.542	0.2261
	Duration	0.004	<0.0001
	FPI	1.733	0.0410
	Wind direction	-0.025	0.0525

Table 9. Summary of analysis explanatory variables for  $\delta D$  model

<b>Term</b>	<b>R2</b>	<b>Estimate</b>	<b>p-value</b>
Duration	0.082	-0.002	0.2342
Relative humidity	0.630	482.5	<0.001
Temperature	0.144	-3.179	0.1093
Wind speed	0.041	-0.844	0.9901
Wind direction	0.022	0.083	0.5459
Wind deviation	0.026	0.135	0.5107
FPI	0.528	14.26	0.0004

Table 10. Summary of analysis of explanatory variables for  $\delta^{18}\text{O}$  model.

Term	R2	Estimate	p-value
Duration	0.008	5.6E-5	0.7157
Relative humidity	0.378	54.82	0.0051
Temperature	0.302	-0.611	0.0149
Wind speed	0.434	-0.276	0.0022
Wind direction	0.264	-0.028	0.0245
Wind deviation	0.113	0.020	0.1588
FPI	0.427	1.750	0.0024

Table 11. Multivariate linear regression model output for stable isotopic  $\delta^2\text{H}$  and  $\delta^{18}\text{O}$  values.

$\delta^2\text{H}$ Model				
$R^2$	n	Term	Estimate	p value
0.696	19	Intercept	-519.13	< 0.0001
		Relative humidity	566.09	< 0.0001
		Wind direction	-0.1633	0.0807
$\delta^{18}\text{O}$ Model				
$R^2$	n	Term	Estimate	p value
0.659	19	Intercept	-49.77	0.0012
		Relative humidity	56.08	0.0005
		Wind direction	-0.0292	0.0022